Beam dynamics basics in RF linacs

N. Pichoff
CEA/DIF/DPTA/SP2A/LFPA, France, Nicolas.pichoff@cea.fr

Abstract
After a short introduction to the advantages and drawbacks of linacs versus circular accelerators, the beam acceleration process with RF cavities is explained. Then individual particle motion with time or longitudinal coordinate (longitudinal, non-linear; transverse, periodic-linear) and beam statistical motion (r.m.s. definition, matching, mismatching and emittance growth) are presented.

1 Introduction

This one-hour lecture has been presented at the CERN Accelerator School dedicated to small accelerators in Zeegse, the Netherlands. Its aim is to give to CAS students an introduction to the basics of RF beam dynamics to obtain a good understanding of linacs. Students wanting to learn more about linacs are advised to read books [1] and [2].

After a short introduction on the advantages/drawbacks of linacs versus circular accelerators, the two main functions are presented:

- Beam *acceleration with RF cavities*. Many configurations of electromagnetic fields can oscillate with their own frequency in a cavity. These modes are excited by the RF source or the beam itself. In nominal conditions, only one mode, whose electric field is along beam propagation, is excited by the RF source. The energy gain of a cavity can be obtained from a simple model using the cavity voltage, an average phase and a correction coefficient called the transit time factor. Moreover, different types of cavities (sections) are used depending on their acceleration efficiency at a given energy (given by the effective shunt impedance). Finally, for a proper acceleration, these cavities have to be synchronized with the beam.

- Beam *transport in a periodic confinement*. In order to reduce emittance growth along the linac, the total phase-space swept by the beam has to be as small as possible. This is obtained by putting cavities (for acceleration and longitudinal focusing) and quadrupoles (for transverse focusing) in accelerating sections composed of periodic lattices. In each accelerating section, the beam has to be matched at entrance allowing a periodic motion of its envelope. Between accelerating sections, dedicated matching sections can be used to re-match the beam because of the change of lattice.

In order to be coherent with the reader, some notions which were not presented in the short one-hour lecture are exposed in the paper. However, these notions were introduced in other lectures in this school, in particular by Alessandra Lombardi in her lecture *Transverse dynamics* I *Beam lines* and Joel Leduff in his lecture *Longitudinal beam dynamics and stability*.

2 Why RF linacs?

The goal of a particle accelerator is to set a *wanted* beam within a *lower cost*. By *wanted*, one means a given particle type, with a given intensity, at a given energy within a given emittance (or brightness)

in a given time structure. The *cost* should include the construction as well as the operation costs (including the staff).

The three main competitors fulfilling this goal are synchrotrons, cyclotrons, and RF linear accelerators (linacs)[1].

The main advantages of linacs over other competitors are

- they can handle *high-current* beams (they are not, or less limited by tune shift);
- they can run in *high duty-cycle* (the beam passes only once at each position);
- they exhibit *low synchrotron-radiation losses* (no dipoles).

Their main drawbacks are

- they are very space and cavity consuming;
- the synchrotron radiation damping of light particles (electrons/positrons) cannot be easily used to reduce the native beam emittance.

That is why the linacs are mainly used

- as low-energy injectors (where the space-charge force is more important and the duty-cycle is high);
- with high-intensity/power beams (high space-charge level or/and duty cycle);
- in new lepton collider project at very high energy (no radiation losses).

3 Beam acceleration with RF cavities

The role of an RF cavity is to give energy to the beam. As the RF represents generally the major part of the cost of a linac structure (except the building), the RF structure has to be chosen, studied, and optimized very carefully. In this lecture, only the principle of an RF cavity is presented. More precise information can be found in the CAS sections dedicated to RF [3].

The principle of travelling-wave cavities usually used for acceleration of ultra-relativistic beams is presented in **Section 3.1**.

The mostly used standing-wave cavity is then presented in **Section 3.2**. Excitation of resonant modes is explained (**3.2.1**). A simple model of energy gain, including the cavity voltage, the particle average phase and its transit time factor calculation is presented (**3.2.2**). The effective shunt impedance quantifying the efficiency of the different cavities helps to choose between different types of accelerating structures (**3.2.3**).

Finally, **Section 3.3** shows the way to calculate the relative phases between all the cavities to accelerate the beam as chosen by the linac designers.

3.1 Travelling-wave cavity

Travelling-wave cavities are mostly used to accelerate ultra-relativistic particles. These cavities generally have two power ports. One from which the power enters, the other, at the other end, through which the power exits (Fig. 1). The electric field travels through the cavity from the input to the output port. Its phase velocity is matched to the beam velocity. The field phase is chosen to continuously accelerate the beam.

[1] We should not forget electrostatic machines, suitable for low-current, low-energy beams.

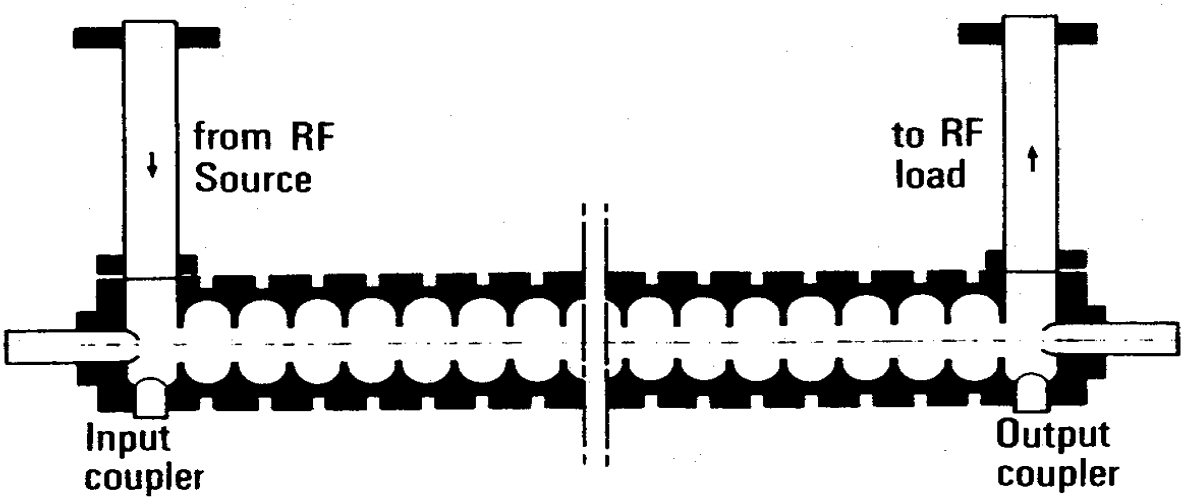

Fig. 1: A travelling-wave cavity

The RF phase velocity in empty cavities or wave-guides is usually higher than (or equal to) the speed of light in vacuum *c*. As particle velocity cannot exceed *c*, the RF phase velocity should be slowed down to reach the synchronism condition. This can be done by introducing some periodic obstacles into the guide (such as an iris-loaded waveguide). The periodic field can then be expanded in a Fourier series, with different wave numbers:

$$Ez(t,z) = \sum_{n=-\infty}^{+\infty} ez_n \cdot \exp\left(j \cdot (\omega t - k_n z)\right). \tag{1}$$

Here ez_n are the ***space harmonic*** amplitude, k_n are the space harmonic wave numbers,

$$k_n = k_0 + \frac{2\pi n}{d}, \tag{2}$$

d is the obstacle period, and $\boldsymbol{k_0}$ is the guide wave number. The phase velocity $\boldsymbol{v_n}$ of space-harmonic number *n* is

$$v_n = \frac{\omega}{k_n}. \tag{3}$$

A particle, whose velocity is close to the phase velocity of one space harmonic, exchanges energy with it. Otherwise, the average effect is null.

A complete calculation of these insertion obstacles as well as a large bibliography can be found in Ref. [4]. This kind of travelling-wave accelerating structure is mainly used to accelerate ultra relativistic electrons. These cavities are explained in more detail in Maurizio Vretenar's lecture *Differences between electron and ion linacs.*

The model of travelling-wave acceleration, even when accelerating with standing-wave cavities, is often used to simplify the calculation of equations of longitudinal motion.

3.2 Standing-wave cavity

3.2.1 Field calculation

An RF cavity is simply a piece of conductor enclosing an empty volume (generally vacuum). Solutions of Maxwell's equations in this volume, taking into account the boundary conditions on the conductor surface, allow the existence of electromagnetic field configurations in the cavity: the *resonant modes*.

$$\vec{\nabla}\cdot\vec{E}=\frac{\rho}{\varepsilon_0}, \qquad \vec{\nabla}\cdot\vec{B}=0,$$

$$\vec{\nabla}\times\vec{E}=-\frac{\partial\vec{B}}{\partial t}, \qquad \vec{\nabla}\times\vec{B}=\mu_0\vec{J}+\frac{1}{c^2}\cdot\frac{\partial\vec{E}}{\partial t}.$$

$\mu_0 = 4\pi\cdot10^{-7}$ T.m.A^{-1} : permeability of free space,
$\varepsilon_0 = 1/\mu_0 c^2$: permittivity of free space,
c = 299,792,458 m.s^{-1} : speed of light in vacuum.

Maxwell's equations

$$\vec{n}\times\vec{E}_n=\vec{0}, \qquad \vec{n}\cdot\vec{B}_n=\vec{0},$$

$$\vec{n}\cdot\vec{E}_n=\frac{\Sigma}{\varepsilon_0}, \qquad \vec{n}\times\vec{H}_n=\vec{K}.$$

$\vec{n}$, the normal to the conductor,
Σ (C/m^2), the surface charge density,
$\vec{K}$ (A/m), the surface current density.

Boundary conditions

Each mode, labelled *n*, is characterized by an electromagnetic field amplitude space configuration $\vec{E}_n(\vec{r})/\vec{B}_n(\vec{r})$ (see DTL example on Fig. 2) oscillating with an RF frequency f_n. The electric field amplitude configuration is the solution of the equation

$$\vec{\nabla}^2\vec{E}_n+\frac{\omega_n^2}{c^2}\cdot\vec{E}_n=\vec{0}, \tag{4}$$

where $\vec{E}_n(\vec{r})$ should satisfy the boundary conditions, $\omega_n=2\pi\cdot f_n$ is the mode pulsation.

The electric (as well as magnetic) field in the cavity at a given time is a weighted sum of the contribution of all the modes:

$$\vec{E}(\vec{r},t)=\sum e_n(t)\cdot\vec{E}_n(\vec{r})=\sum a_n\cdot e^{j\omega_n t}\cdot\vec{E}_n(\vec{r}). \tag{5}$$

Here a_n is a complex number, $e_n(t)$ is the field variation with time, solution of [5]:

$$\ddot{e}_n+\omega_n^2\cdot e_n=-\frac{\omega_n^2}{\sqrt{\varepsilon\mu}}\cdot\int_S\left(\vec{E}\times\vec{H}_n\right)\cdot\vec{n}\cdot dS + \frac{1}{\varepsilon}\frac{d}{dt}\int_{S'}\left(\vec{H}\times\vec{E}_n\right)\cdot\vec{n}\cdot dS'-\frac{1}{\varepsilon}\frac{d}{dt}\int_V\vec{J}(\vec{r},t)\cdot\vec{E}_n(\vec{r})\cdot dV \tag{6}$$

$\vec{H}$ is the magnetic induction,

$\vec{J}$ is the current density, of the beam for example,

S is the conductor inside surface,

S' is the open surface of the cavity,

V is the inside volume of the cavity.

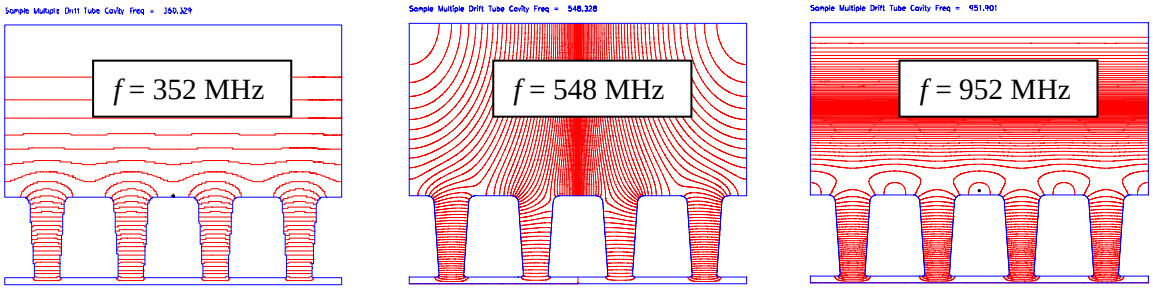

Fig. 2: Three RF mode configurations in a four-gap DTL (D. Uriot, CEA/DSM)

– The first term on the right-hand side is an integral over the conductor surface. Because of power losses by Joule effects on this non-perfect conductor, it can be modelled by a damping term:

$$-\frac{\omega_n}{Q_{0n}}\cdot\dot{e}_n\,. \tag{7}$$

The calculation of $\boldsymbol{Q_{0n}}$, the *quality factor of the mode*, can be deduced from power loss considerations:

$\boldsymbol{U_n(0)}$ is the energy stored by the *n*-mode at time $t = 0$. For $t > 0$, no more power is injected in the cavity. Let us define $\boldsymbol{k(t)}$ as the ratio between the field amplitude at *t* and this at $t = 0$:

$$k(t)=\frac{e_n(t)}{e_n(t=0)}\,. \tag{8}$$

The energy lost per unit time is the power dissipated in the conductor $\boldsymbol{P_n}$:

$$\frac{dU_n(t)}{dt}=-P_n(t)\,. \tag{9}$$

The average power dissipated in the conductor per cycle is proportional to the square of the current density (and then the magnetic field) close to the surface:

$$P_n=\frac{R_s}{2}\int_S K_n^2\,dS=\frac{R_s}{2}\int_S H_n^2\,dS\,, \tag{10}$$

where $\boldsymbol{R_s}$ is the surface resistance defined as:

$$R_s=\sqrt{\frac{\mu_0\pi f_0}{\sigma}}\,,\ \text{for } \textit{normal conductors} \tag{11}$$

$\boldsymbol{\sigma}$ is the conductivity ($1/\sigma = 1.7\cdot10^{-7}$ Ω.m for copper).

$$R_s\approx R_{\text{res}}+9\cdot10^{-5}\frac{f_0^2\,(\text{GHz})}{T\,(\text{K})}\exp\left(-1.92\cdot\frac{T_c}{T}\right),\ \text{for } \textit{superconducting niobium} \tag{12}$$

Here $\boldsymbol{R_{res}}$ is the residual resistance (10^{-9}–10^{-8} Ω) depending on the surface imperfections,

$\boldsymbol{T}$ is the working absolute temperature,

$\boldsymbol{T_c}$ = 9.2 K is the critical temperature.

From equations (8) and (10) can be deduced

$$P_n(t) = k(t)^2 \cdot P_n(t=0). \tag{13}$$

The stored energy is proportional to the square of the field:

$$U_n = \frac{\varepsilon_0}{2} \iiint \left\| \vec{E}_n \right\|^2 dv = \frac{1}{2\mu_0} \iiint \left\| \vec{B}_n \right\|^2 dv \ , \tag{14}$$

giving:

$$U_n(t) = k(t)^2 \cdot U_n(t=0). \tag{15}$$

Equation (9) becomes

$$\frac{dk^2}{dt} = -\frac{P_{n0}}{U_{n0}} \cdot k^2 = 2 \cdot k \cdot \dot{k}\,, \tag{16}$$

giving the time evolution of the electric field amplitude:

$$\frac{de_n}{dt} = -\frac{P_{n0}}{2 \cdot U_{n0}} \cdot e_n\,, \tag{17}$$

whose solution is

$$e_n(t) = e_n(0) \cdot \exp\left(-\frac{P_n}{2 \cdot U_n} \cdot t \right). \tag{18}$$

A comparison with the damping term of a second-order linear differential equation written in (7):

$$\ddot{e}_n + 2 \cdot \alpha \cdot \dot{e}_n + \omega_n^2 \cdot e_n = 0\,, \tag{19}$$

whose solution is

$$e_n(t) = e_n(0) \cdot \exp(-\alpha \cdot t) \cdot \cos\left(\sqrt{\omega_n^2 - \alpha^2} \cdot t \right)\,, \tag{20}$$

gives

$$\boxed{Q_{0n} = \frac{\omega_n \cdot U_n}{P_n}}\,. \tag{21}$$

– In the second term, the integration is performed over the open surfaces *S′* and represents the coupling of the cavity with the outside. This coupling can be divided into two contributions:

the injected power coming from the power generator through the coupler,

an additional damping, which can be represented by another quality factor $\boldsymbol{Q_{exn}}$ known as the ***external Q,*** corresponding to power losses through the opened surfaces.

The coupling can be calculated from the coupler geometry with electromagnetic codes. This second term can then be written:

$$-\frac{\omega_n}{Q_{exn}}\cdot\dot{e}_n + S_n\cdot e^{j(\omega_{RF}t+\varphi_0)}. \tag{22}$$

Here $S_n\cdot e^{j(\omega_{RF}t+\varphi_0)}$ is the RF source filling through the coupler.

– The last term, represents the field excited by the beam, known as the ***beam loading***. It is proportional to the beam intensity:

$$k_n\cdot\underline{I}(t). \tag{23}$$

$\underline{I}(t)$ is a complex number (it has an amplitude and a phase) representing the beam current.

Equation (6) can finally be modelled by

$$\boxed{\frac{d^2e_n}{dt^2}+\frac{\omega_{\mathrm{RF}}}{Q_n}\cdot\frac{de_n}{dt}+\omega_n^2\cdot e_n = S_n\cdot e^{j(\omega_{\mathrm{RF}}t+\varphi_0)}+k_n\cdot\underline{I}(t)}, \tag{24}$$

which is the equation of a damped harmonic oscillator in a forced regime.

Q_n is the quality factor of the cavity, with

$$\frac{1}{Q_n}=\frac{1}{Q_{0n}}+\frac{1}{Q_{exn}}, \tag{25}$$

$$\tau = 2\cdot\frac{Q_n}{\omega_{\mathrm{RF}}}$$

is the cavity filling time.

One notes that both the coupler and the beam can excite some RF modes.

Equation (24) is of an RLC circuit which is often used to model the system. A complete study of this model, out of the scope of this lecture, can be found in Ref. [5].

Among all these modes, one, having an electric field on-axis along the longitudinal direction, is used to accelerate the beam. The cavity geometry is calculated to match the frequency of this accelerating mode up to the RF frequency. This mode is excited in the cavity through the power coupler whose geometry is calculated and adjusted to transfer electromagnetic energy in the cavity to the beam without reflection (this procedure is called coupler matching).

3.2.2 Energy gain model in a standing-wave cavity

A cavity has a finite length $\boldsymbol{L}$. $\boldsymbol{s_0}$ is the cavity input abscissa. $\boldsymbol{E_z(s)}$ is the amplitude of the electric field longitudinal component on axis.

The energy[2] gained by a charged particle on-axis in the cavity is

$$\Delta W = \int_{s_0}^{s_0+L} qE_z(s)\cdot\cos(\phi(s))\cdot ds, \tag{26}$$

where $\boldsymbol{q}$ is the particle charge,

[2] This is actually the longitudinal energy, but we can consider that there is no transverse field on cavity axis.

$\phi(s)$ is the cavity RF phase when the particle is at abscissa s. It is defined as

$$\phi(s) = \phi_0 + \frac{\omega}{c}\int_{s_0}^{s_0+s}\frac{ds'}{\beta_z(s')} \tag{27}$$

where $\phi_0 = \phi(s_0)$ is the RF phase when the particle enters the cavity.

Writing $\phi(s) = \phi(s) + (\phi_s - \phi_s)$, ϕ_s being an arbitrary phase and using trigonometric relationships, one gets for the energy gain:

$$\Delta W = \cos\phi_s \cdot \int_{s_0}^{s_0+L} qEz(s)\cdot\cos(\phi(s)-\phi_s)\cdot ds - \sin\phi_s \cdot \int_{s_0}^{s_0+L} qEz(s)\cdot\sin(\phi(s)-\phi_s)\cdot ds. \tag{28}$$

By defining ϕ_s as

$$\int_{s_0}^{s_0+L} qEz(s)\cdot\sin(\phi(s)-\phi_s)\cdot ds = 0\,,$$

giving the definition of the ***average phase*** ϕ_s (also called synchronous phase),

$$\boxed{\phi_s = \arctan\left(\frac{\int_{s_0}^{s_0+L} Ez(s)\cdot\sin\left[\phi(s)\right]\cdot ds}{\int_{s_0}^{s_0+L} Ez(s)\cdot\cos\left[\phi(s)\right]\cdot ds}\right)}, \tag{29}$$

one finally gets

$$\boxed{\Delta W = qV_0\cdot T\cdot\cos\phi_s}, \tag{30}$$

with

$$\boxed{V_0 = \int_{s_0}^{s_0+L}\left|Ez(s)\right|\cdot ds}. \tag{31}$$

$\boldsymbol{V_0}$ is the *cavity voltage*. $q\cdot V_0$ represents the maximum energy (in eV) that a particle with charge q could gain if the field were always maximum.

$$\boxed{T = \frac{1}{V_0}\int_{s_0}^{s_0+L} Ez(s)\cdot\cos(\phi(s)-\phi_s)\cdot ds}. \tag{32}$$

$\boldsymbol{T}$ is known as the ***transit time factor***. It depends on the *particle initial velocity as well as on the field amplitude.* It can be noted that this definition does not make any assumption about the field shape (no symmetry) resulting from a slightly different average phase definition which can be found in the literature (which is often taken as the RF phase when the particle reaches the mid-cavity). When the velocity gain in the cavity is much lower than the input particle velocity, T depends only on the velocity and can be easily tabulated.

The transit time factor T is difficult to calculate using formula (32) as ϕ_s has to be known. In fact, T does not depend on ϕ_s when the velocity gain in the cavity is small. The transit time factor is then the maximum energy that can be gained in the cavity normalized to the cavity voltage. This maximum energy gain is simply the modulus of the complex number whose real part represents the energy gain:

$$\boxed{T = \frac{1}{V_0}\left|\int Ez(s)\cdot e^{j\phi(s)}\cdot ds\right|}. \tag{33}$$

3.2.3 Shunt impedances

At first order, one considers that only one mode, the accelerating mode, is excited in the cavity. The transverse component of the electric field is generally null on the axis. An expression of the field z-component on the axis is then

$$E_z(s,t) = E_{z0}(s)\cdot\cos(\omega t+\varphi). \tag{34}$$

Here $E_{z0}(s)$ is the field amplitude.

Let $\boldsymbol{P_d}$ be the *power deposition in the cavity*. It can be modelled by

$$P_d = \frac{V_0^2}{2\cdot R}, \tag{35}$$

where $\boldsymbol{V_0}$ is the cavity voltage.

$\boldsymbol{R}$ is known as the *cavity shunt impedance* and is very useful in cavity design. For an optimal acceleration, it has to be the highest possible.

As for the quality factor Q, the shunt impedance R is linked to the energy lost in the cavity.

One can easily show that the '*R over Q*' factor depends only on the geometry of the cavity:

$$\frac{R}{Q} = \frac{V_0^2/2\cdot P_d}{\omega\cdot U/P_d} = \frac{V_0^2}{2\cdot\omega\cdot U}, \tag{36}$$

as Eq. (14) shows that $U \propto V_0^2$.

One can easily see that, for the same aspect ratio, doubling the frequency (corresponding to divided by 2 the cavity length and by 8 its volume), has no effect on the cavity '*R* over *Q*'.

Generally, because the electric field is changing with time as the particle transits through the cavity, the maximum energy, $q\cdot V$, which can be gained in the cavity by a particle of charge q is lower than $q\cdot V_0$. One defines the *transit time factor* $\boldsymbol{T}$ as:

$$T = \frac{V}{V_0} \le 1. \tag{37}$$

It is a corrective factor on the energy gain taking into account the particle transit time in the cavity. It obviously depends on the particle velocity.

The *effective shunt impedance* $\boldsymbol{RT^2}$ is then proportional to the ratio between the square of the maximum energy $\Delta U_{\max}$ that can be gained by the beam and the power lost in the cavity:

$$RT^2 = \frac{\Delta U_{\max}^2}{2P_d}. \tag{38}$$

It is some sort of cavity efficiency and has to be maximized.

The effective shunt impedance is often used to compare the efficiency of different structures at a given energy. As their geometries are generally different, one extends the preceding definition per unit length to allow a better comparison.

Let $\boldsymbol{L}$ be the cavity length[3]. The cavity average electric field $\boldsymbol{E_0}$ is defined as

$$E_0 = \frac{V_0}{L}. \tag{39}$$

The power deposition per unit length in the cavity $\boldsymbol{P'_d}$ is then

$$P'_d = \frac{E_0^2}{2 \cdot Z}, \tag{40}$$

where $\boldsymbol{Z}$ is the cavity shunt impedance per unit length.

The effective shunt impedance per unit length $\boldsymbol{ZT}^2$ is then proportional to the ratio between the square of the maximum energy $\Delta U'_{\max}$ that can be gained per unit length by the beam and the power lost per unit length in the cavity:

$$ZT^2 = \frac{\Delta U'^2_{\max}}{2P'_d}. \tag{41}$$

As it depends on the particle velocity, one chooses the structure that maximizes ZT^2 at a given energy. Figure 3 represents the evolution of the effective shunt impedance per metre for two different proton linac structures (SDTL and CCL) with different apertures ϕ. The higher the aperture (room for beam) the lower the effective shunt impedance. SDTL structures are more efficient at lower energy as CCL structures are more efficient at higher energy. In this case, the optimum transition energy is around 100 MeV for protons.

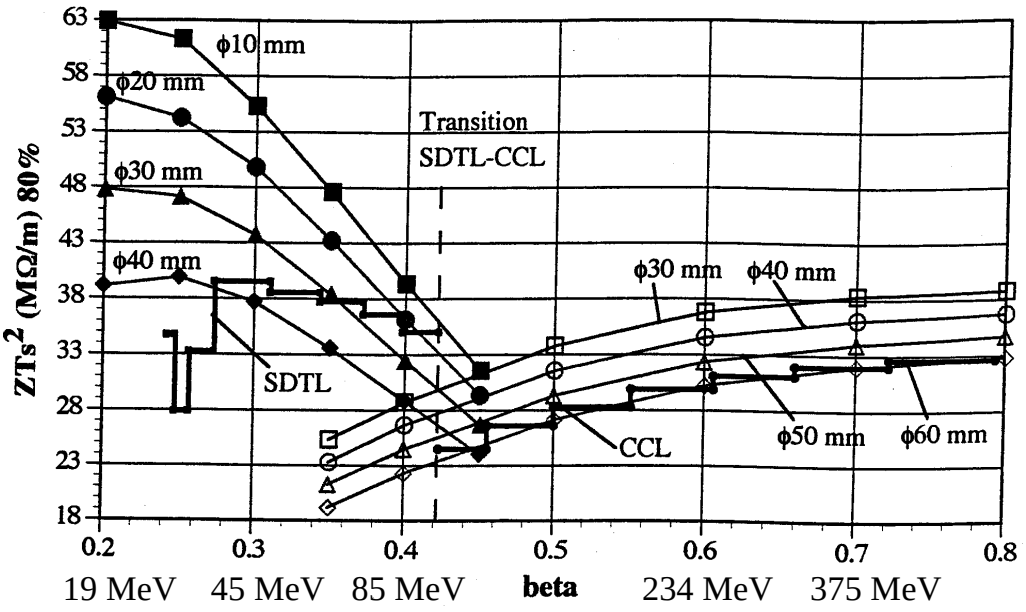

Fig. 3: Effective shunt impedance per metre of different structures (TRISPAL, C. Bourrat)

[3] On account of the cavity fringe field, *L* is often arbitrarily defined as the physical length of the cavity.

3.3 Notion of synchronism

A linac is designed such that one *theoretical particle*, called the ***synchronous particle***, enters successively on axis of RF cavities with a designed RF phase law in order to get a wanted energy gain. This very important notion of synchronism allows understanding the efficiency as well as the stability of the linacs.

Particles can be accelerated with travelling waves as well as standing waves.

3.3.1 With travelling waves

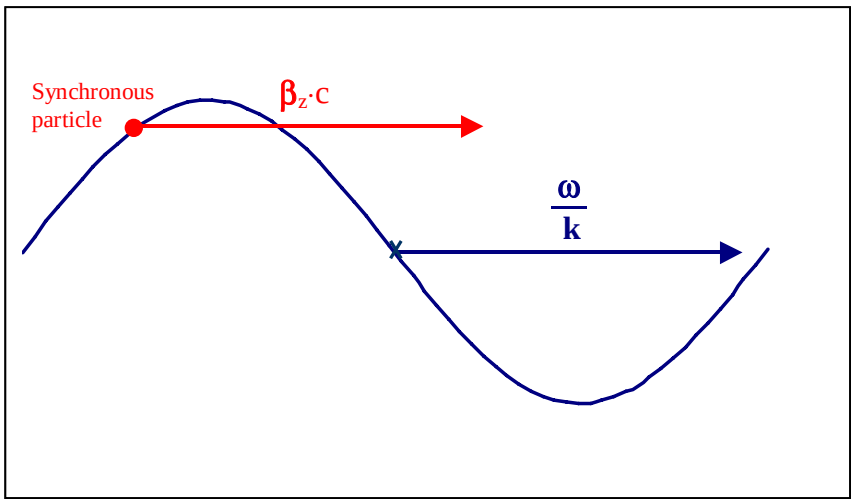

Fig. 4: Particle accelerated by a travelling wave

The on-axis RF accelerating field in a travelling-wave cavity can be written as

$$E_z(z,t) = E_0 \cdot \cos(\omega t - kz), \tag{42}$$

where ω is the RF pulsation, and k is the RF wave number (Fig. 4).

The synchronism condition is reached when the particle longitudinal velocity equals the RF phase velocity:

$$\beta_z c = \frac{k}{\omega}. \tag{43}$$

Here c is the speed of light in vacuum, β_z is the reduced longitudinal velocity of the synchronous particle. It can be noted that when the *paraxial approximation*[4] is used, β_z is replaced by β, the reduced total speed of the particle.

3.3.2 With standing waves

In most linacs, the beam is accelerated with RF cavities or gaps operating in standing-wave conditions. An RF power, produced by one or many RF sources, is introduced through a coupler in a resonant cavity exciting the wanted standing-wave accelerating mode. The cavity shape has been calculated and adjusted to match the accelerating mode to the power-supply frequencies and to throw the other mode frequencies far from the RF one.

[4] As $\beta = \beta_z \cdot \sqrt{1 + x'^2 + y'^2}$, the paraxial approximation occurs when $x' << 1$ and $y' << 1$.

As a first step, let us assume a set of thin independently phased RF cavities along the beam path (Fig. 5).

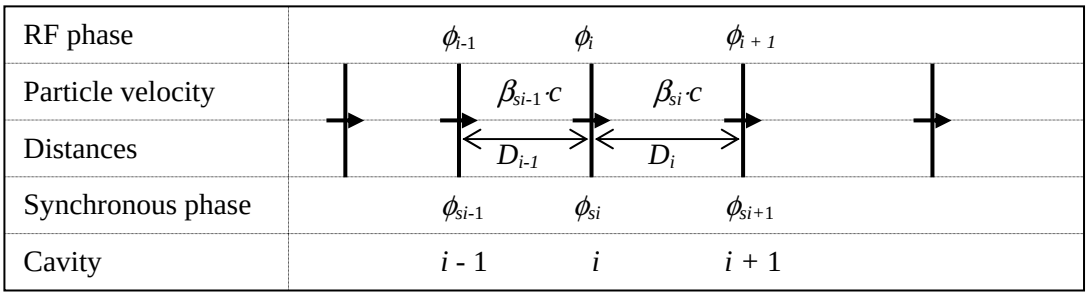

Fig. 5: A set of independently phased cavities

ϕ_i is the absolute RF phase in the ith cavity when $t = 0$ (the $t = 0$ instant has been arbitrarily chosen),

β_{si} is the synchronous particle reduced velocity at the ith cavity output,

ϕ_{si} is the RF average phase of the ith cavity of the synchronous particle,

D_i is the distance between the ith and the $i + 1$th cavities.

The synchronism condition is reached when the RF phase difference between two consecutive cavities, $\Delta\phi_i = \phi_{i+1} - \phi_i$, equals the phase evolution during synchronous particle time of flight between both cavities,

$$\omega \cdot \frac{D_i}{\beta_{si} \cdot c} = 2\pi \cdot \frac{D_i}{\beta_{si}\lambda},$$

plus the difference $\Delta\phi_{si} = \phi_{si+1} - \phi_{si}$ between the designed synchronous phase in each cavity:

$$\Delta\phi_i + [2\pi \cdot n] = \Delta\phi_{si} + 2\pi \cdot \frac{D_i}{\beta_{si}\lambda}. \tag{44}$$

$\lambda = c/f$ is the RF wavelength.

One observes that the synchronism condition does not depend on the RF field amplitude. It has a non-intuitive consequence: an increase of the accelerating field amplitude in the cavities without phase change does not induce an increase of the synchronous particle final energy but a change of the synchronous phase fulfilling the synchronism condition.

Two different kinds of structure exist:

– *Coupled cavity structures* where the phase between consecutive cavities is fixed. The synchronism condition is achieved by adjusting the distance between the cavities.

  In a Drift Tube Linac (DTL), for example, the phase difference between the cells is fixed (= 2π). The distance between cells is then calculated to get

$$D_i = \left(\frac{\Delta\phi_{si}}{2\pi} + 1\right) \cdot \beta_{si}\lambda. \tag{45}$$

– *Independent cavity structures* where the distance between cavities is fixed. The synchronism condition is then achieved by adjusting the phase difference between the cavities.

In a Superconducting Cavity Linac (SCL), for example, the distance between cavities is fixed by the cryogenics mechanics (as small as technologically possible). The phase difference between cavities is then calculated to have

$$\Delta\phi_i = \Delta\phi_{si} + 2\pi \cdot \frac{D_i}{\beta_{si}\lambda} + [2\pi n]. \tag{46}$$

4 Beam transport

A beam is a set of particles. The beam motion can then be expressed as the statistical result of the motion of individual particles. Many codes are now transporting beam particles individually, reconstructing beam properties where they are needed.

The first step is to study individual particle motion in the accelerator (**Section 4.1**). This motion can be expressed by the variation of the particle coordinates with time (**4.1.1**) or with longitudinal position along the linac (**4.1.2**). The non-linear dynamics along the longitudinal direction (**4.1.3**) is traditionally separated from the linear and periodic transverse dynamics (**4.1.4**), despite a more or less influent coupling.

The second step consists in constructing a beam as statistical properties of a cloud (or distribution) of particles, in particular through its emittance (**4.2.1**) and r.m.s. properties (**4.2.2**). For a proper beam transport, these beam properties have to be matched to the linac (**4.2.3**) to avoid degradation of the beam optical properties along the transport through the linac.

4.1 Particle motion

4.1.1 General equation of motion with time

Electromagnetic fields can be divided into two contributions:

– the electric field: $\vec{E}$,

– the magnetic field: $\vec{B}$.

The intensity of these contributions depends on the referential where they are expressed.

The equation of motion of a particle of charge q in these fields is:

$$\frac{d\vec{p}}{dt} = q \cdot \left(\frac{\vec{p}}{\gamma \cdot m} \times \vec{B}(t,\vec{r}) + \vec{E}(t,\vec{r}) \right). \tag{47}$$

Here $\vec{p}$ is the momentum of the particle, m its mass, γ its reduced energy, $\vec{r}$ its position.

Using the reduced momentum,

$$\gamma\vec{\beta} = \frac{\vec{p}}{m \cdot c},$$

one gets

$$\frac{d\gamma\vec{\beta}}{dt} = \frac{Z \cdot c}{mc^2/e} \cdot \left(\frac{\gamma\vec{\beta}}{\gamma} \times c\vec{B}(t,\vec{r}) + \vec{E}(t,\vec{r}) \right). \tag{48}$$

Here c is the velocity of light in vacuum, mc^2/e is the particle rest mass in eV, Z is the particle charge number.

It is convenient to multiply the magnetic field by c because it is homogeneous to an electric field. In that case a magnetic field of 1 T is 'equivalent' to an electric field of 300 MV/m.

The particle reduced energy γ can be deduced from its reduced momentum:

$$\gamma = \sqrt{1 + \left\| \gamma\vec{\beta} \right\|^2} \ . \tag{49}$$

The variation of the position is given by

$$\frac{d\vec{r}}{dt} = \frac{\gamma\vec{\beta}}{\gamma} \cdot c \ . \tag{50}$$

The motion of each particle can be described using only two vectors (six coordinates): $\left(\vec{r}, \gamma\vec{\beta}\right)$.

The new generation of codes uses time more and more as an independent variable. It is particularly the case for simulations of RF guns, RFQs or beams with strong space-charge. Moreover, Maxwell's equations can be solved with time to compute the evolution of the electromagnetic field and be coupled with the particle's motion.

Nevertheless, because of the particularity of accelerators that have a privileged axis, because transport elements are placed at given positions along the beam path and because diagnostics measuring beam properties are also placed at given positions, time is replaced in 'traditional' beam dynamics by the longitudinal position in the accelerator as independent variable.

4.1.2 Equation of motion with longitudinal position

4.1.2.1 General equations

Let us call ***s*** the longitudinal position (abscissa) in the linac path (rather than z to avoid any confusion with the particle longitudinal position in the bunch at a given time), the equation of motion (47) can be rewritten:

$$\frac{d\vec{p}}{ds} = q \cdot \frac{\vec{v} \times \vec{B} + \vec{E}}{v_z} \ , \tag{51}$$

$$v_z = \frac{ds}{dt} \ ,$$

where v_z is the particle longitudinal velocity.

Using reduced momentum and convenient physical parameters, one gets

$$\frac{d\gamma\vec{\beta}}{ds} = \frac{Z}{mc^2/e} \cdot \frac{\vec{\beta} \times c\vec{B} + \vec{E}}{\beta_z} \ , \tag{52}$$

c is the velocity of light in vacuum, mc^2/e is the particle rest mass in eV, Z is the particle charge number.

A projection on a Cartesian frame[5] (x, y, z) gives

[5] In general, x and y play the same role in a linac (in contrast with that of a circular accelerator).

$$\boxed{\begin{cases} \dfrac{d\gamma\beta_x}{ds} = \dfrac{Z}{mc^2/e}\cdot\left(y'\cdot cB_z - cB_y + \dfrac{E_x}{\beta_z}\right) = \dfrac{d\gamma\beta_z x'}{ds} \\ \dfrac{d\gamma\beta_y}{ds} = \dfrac{Z}{mc^2/e}\cdot\left(cB_x - x'\cdot cB_z + \dfrac{E_y}{\beta_z}\right) = \dfrac{d\gamma\beta_z y'}{ds} \\ \dfrac{d\gamma\beta_z}{ds} = \dfrac{Z}{mc^2/e}\cdot\left(x'\cdot cB_y - y'\cdot cB_x + \dfrac{E_z}{\beta_z}\right) \end{cases}} \tag{53}$$

$$x' = \frac{dx}{ds} = \frac{p_x}{p_z} = \frac{\beta_x}{\beta_z} \qquad \text{and} \qquad y' = \frac{dy}{ds} = \frac{p_y}{p_z} = \frac{\beta_y}{\beta_z}$$

are the *slopes* of the particle;

$$\beta_w = \frac{v_w}{c},$$

the reduced velocity *w*-component; *w* being *x*, *y* or *z*; v_w being the particle velocity *w* component; *m* and *q* are, respectively, the rest mass and the charge of the particle; *c* is the speed of light.

One clearly observes that *longitudinal and transverse motions are coupled*. However, for an easier understanding, and because the coupling is often very weak, the longitudinal and the transverse motions are usually treated as uncoupled, the longitudinal velocity v_z variations being considered apart. To uncouple the transverse and longitudinal motions, the ***paraxial approximation*** has to be done.

4.1.2.2 Paraxial approximation

The *paraxial approximation* consists in assuming that the velocity of the particles is mainly along the longitudinal direction, i.e., the slopes of the particle are very small:

$$x'^2 + y'^2 << 1. \tag{54}$$

Its natural consequence is that the longitudinal velocity or momentum can be assimilated to the total velocity or momentum:

$$\beta_z = \beta\cdot\sqrt{1 + x'^2 + y'^2} \approx \beta\,. \tag{55}$$

For example, if x' < 100 mrad and y' < 100 mrad, the error on β (or β_z) is lower than 1%.

This approximation is very good at high energy where the beam divergence is small, but is sometime more difficult to justify at very low energy.

4.1.2.3 Energy gain calculation

From Eqs. (53) and (49), one can easily obtain the energy gain:

$$\frac{d\gamma}{ds} = \beta_z\left(x'\cdot\frac{d\gamma\beta_x}{ds} + y'\cdot\frac{d\gamma\beta_y}{ds} + \frac{d\gamma\beta_x}{ds}\right), \tag{56}$$

giving

$$\boxed{\frac{d\gamma}{ds} = \frac{q}{mc^2}\cdot\left(x'E_x + y'E_y + E_z\right)}. \tag{57}$$

One finds the well-known result that the magnetic field does not contribute to energy gain.

4.1.3 Longitudinal particle dynamics (motion in non-linear force)

4.1.3.1 The longitudinal variables

The variables generally used to describe the longitudinal particle motion, as a function of *s*, are

- ϕ, the absolute particle phase, calculated from the RF frequency, with $\phi = 0$ arbitrarily chosen;
- W, the particle kinetic energy[6].

The evolution of ϕ and W with s is given by the equations

$$\begin{cases} \dfrac{d\phi}{ds} = \dfrac{\omega_{\mathrm{RF}}}{\beta_z c} = \dfrac{2\pi}{\beta \cdot \lambda_{\mathrm{RF}} \cdot \sqrt{1 - x'^2 - y'^2}} \\ \dfrac{dW}{ds} = q \cdot \left[x' E_x(s,\phi,r) + y' E_y(s,\phi,r) + E_z(s,\phi,r) \right] \end{cases} . \tag{58}$$

Applying these equations to the synchronous particle, one gets

$$\begin{cases} \dfrac{d\phi_s}{ds} = \dfrac{2\pi}{\beta_s \cdot \lambda_{\mathrm{RF}}} \\ \dfrac{dW_s}{ds} = q \cdot E_z(s,\phi_s,0) \end{cases} . \tag{59}$$

Let us define the ***reduced phase and energy*** variables for each particle:

$$\begin{cases} \varphi = \phi - \phi_s \\ w = W - W_s \end{cases} . \tag{60}$$

All the particles are now referenced to the synchronous particle. Late particles compared to synchronous particle have a positive φ.

The equations of motion of particles with respect to the synchronous particle (with these new variables) become

$$\begin{cases} \dfrac{d\varphi}{ds} = \dfrac{2\pi}{\lambda_{\mathrm{RF}}} \cdot \left(\dfrac{1}{\beta \cdot \sqrt{1 - x'^2 - y'^2}} - \dfrac{1}{\beta_s} \right) \\ \dfrac{dw}{ds} = q \cdot \left[x' E_x(s,\phi,r) + y' E_y(s,\phi,r) + E_z(s,\phi,r) - E_z(s,\phi_s,0) \right] \end{cases} . \tag{61}$$

When the beam is accelerated by a standing-wave cavity structure, synchronous particles enters successive cavities giving it a strong energy gain, separated by long drift spaces where no acceleration occurs. In order to ease the understanding of the physics, this periodic acceleration scheme can be replaced by a continuous acceleration one. This scheme consists in assuming that the beam is accelerated by a travelling wave *propagating at the same speed as that of the synchronous particle*. This scheme allows a mathematical resolution of the dynamics equations[7] with an electric field that does not depend on *s* or *t*.

[6] This is really a 'longitudinal' particle property only in paraxial approximation!
[7] Equations are smoothed for analytic solutions, but quantified for a numerical solution!

4.1.3.2 The continuous electric field model

The electric field, which is generally a function of *s*, is then chosen constant. The field amplitude of the travelling wave is $\boldsymbol{E_0 T}$ (mean electric field) on axis. $\boldsymbol{E_0}$ is defined as the potential gain of one cavity V_0 divided by the distance between the centres of consecutive cavities. The transit time factor $\boldsymbol{T}$ has been included to take into account the variation with the particle velocity of the acceleration in standing-wave cavities.

The on-axis electric field longitudinal component becomes

$$E_z(s,\varphi,r=0) = E_0 T \cdot \cos(\varphi + \phi_{s0}), \tag{62}$$

$\boldsymbol{\phi_{s0}}$ being the RF average phase of the synchronous particle.

The energy gain per metre of the synchronous particle is then

$$G = qE_0 T_s \cdot \cos\phi_{s0}. \tag{63}$$

Here $\boldsymbol{T_s}$ is the transit time factor of the synchronous particle.

Let us assume an *axi-symmetric accelerating field*, the off-axis electric field longitudinal component can be written:

$$E_z(s,\phi,r) = E_0 T \cdot R(r) \cdot \cos(\varphi + \phi_{s0}), \tag{64}$$

with *r* being the radial position of the particle, and $\boldsymbol{R}(r)$ expressing the radial evolution of the electric field longitudinal component. It can usually be written: $R(r) = 1 + O(r^2)$. Close to the axis, Bessel function, a solution of Maxwell's equations in axi-symmetric geometry in vacuum, can be used to express $R(r)$ [6] [2], but far from the axis, the cavity geometry has a strong influence through the boundary conditions. The radial position (r) can be replaced by (x, y) if the cavity is not axi-symmetric. Some authors include the variation of the field with *r* in the transit time factor: *T(r).*

Applying Gauss's law: $\vec{\nabla} \cdot \vec{E} = 0$ and remarking that the electric field transverse component is null on axis, one gets the electric field transverse component:

$$\begin{aligned} E_r(s,\varphi,r) &= -\frac{1}{r} \cdot \int_0^r \frac{\partial E_z(s,\varphi,r)}{\partial s} \cdot r \cdot dr \\ &= -\frac{1}{r} \cdot \frac{E_0 T}{\beta_s \lambda} \cdot \sin(\varphi + \phi_{s0}) \cdot \int_0^r R(r) \cdot r \cdot dr \ . \end{aligned} \tag{65}$$

The electric field radial component can be written

$$E_r(s,\varphi,r) = -\frac{E_0 T}{\beta_s \lambda} \cdot \sin(\varphi + \phi_{s0}) \cdot \left(\frac{r}{2} + O(r^3) \right). \tag{66}$$

4.1.3.3 The simplified equations of motion

Three assumptions should be made to decouple the longitudinal motion from the transverse one:

– Generally, the *paraxial assumption* occurs, and one considers:

$$x'^2 + y'^2 << 1. \tag{67}$$

– In general, one can assume: $r/2 + O\left(r^3\right) << \beta_s \lambda$ and (x', y') << 1. The contribution of the transverse electric field to the energy gain can then be neglected in Eq. (61)[8]:

$$x'E_x + y'E_y << E_z - E_{zs}\,. \tag{68}$$

– Finally, one can assume that the longitudinal field does not depend on the radial position *r*, by taking

$$R(r) \approx 1\,. \tag{69}$$

Using these assumptions, Eqs. (61) become

$$\begin{cases} \dfrac{d\varphi}{ds} = -\dfrac{2\pi}{\lambda}\left(\dfrac{1}{\beta(s)} - \dfrac{1}{\beta_s(s)}\right), \\ \dfrac{dw}{ds} = -q \cdot E_0 T \cdot \left(\cos\phi_{s0} \cdot (1 - \cos\varphi) + \sin\phi_{s0} \cdot \sin\varphi\right) \end{cases} \tag{70}$$

which is in fact the equation of motion of on-axis particles.

Moreover, a small longitudinal velocity dispersion assumption is often made:

$$\frac{1}{\beta} - \frac{1}{\beta_s} = \delta\beta^{-1} << \frac{1}{\beta_s}\,. \tag{71}$$

A *first-order development* around synchronous velocity gives

$$\delta\beta^{-1} = -\frac{w}{(\beta_s\gamma_s)^3 \cdot mc^2}\,. \tag{72}$$

If one considers that the transit-time factor does not depend on the beam particles' energy:

$$T(w) = T_s\,, \tag{73}$$

Eqs. (70) become

$$\begin{cases} \dfrac{d\varphi}{ds} = -2\pi \cdot \dfrac{w}{(\beta_s\gamma_s)^3 \cdot mc^2 \cdot \lambda} = \dfrac{\partial H_{\phi w}}{\partial w} \\ \dfrac{dw}{ds} = -q \cdot E_0 T_s \cdot \left(\cos\phi_{s0} \cdot (1 - \cos\varphi) + \sin\phi_{s0} \cdot \sin\varphi\right) = -\dfrac{\partial H_{\phi w}}{\partial \varphi} \end{cases}. \tag{74}$$

As φ and *w* are canonical variables with the independent variable *s*, a Hamiltonian $\boldsymbol{H_{\varphi w}}$ has been used to describe the particle motion:

$$H_{\varphi w} = -\frac{2\pi}{(\beta_s\gamma_s)^3 \cdot mc^2 \cdot \lambda} \cdot \frac{w^2}{2} - q \cdot E_0 T_s \cdot R(r) \cdot \left[\sin\phi_{s0} \cdot (\cos\varphi - 1) + \cos\phi_{s0} \cdot (\sin\varphi - \varphi)\right]. \tag{75}$$

[8] This assumption is not valid when $\sin\phi_s$ tends to zero (no acceleration). However, when ϕ_s equals 0, even if the transverse kick is the main contributor to energy variation, it is small compared to the energy and always null on the axis.

In the phase space (φ, w), particles are following curves for which $H_{\phi w}$ = C_{st}. They are represented on Fig. 6 for on-axis particles. On Fig. 6(a), $\beta_s\gamma_s$ = C_{st}, as on Fig. 6(a), an adiabatic acceleration ($\beta_s\gamma_s \neq C_{st}$) is added and the bucket turns into the well-known *golf club* shape.

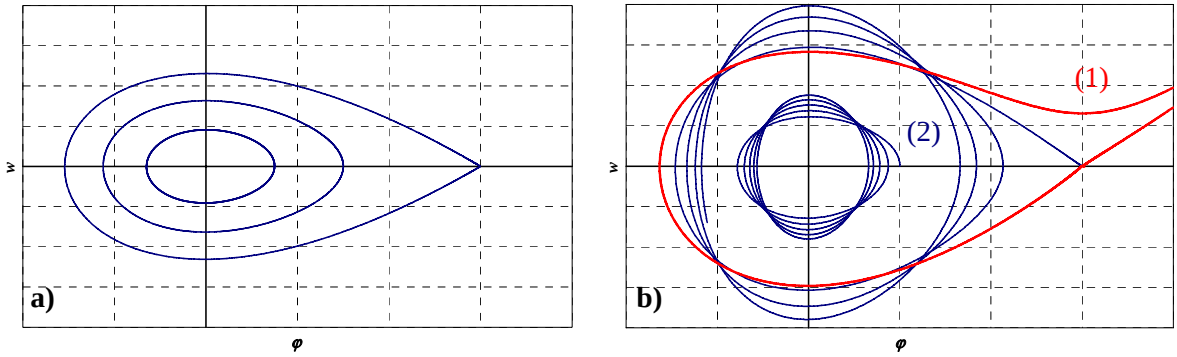

Fig. 6: Particle trajectories in longitudinal phase space

a) $\beta_s\gamma_s = C_{st}$,

b) Adiabatic acceleration: the *golf club* represents the input acceptance [in red, (1)]. In blue (2) are the trajectories of two particles. They exhibit the damping of the phase oscillation amplitude with acceleration.

A particle entering the cavity later than the synchronous particle gets a larger energy gain. A particle entering the cavity earlier gets a smaller energy gain.

The synchronous phase of the synchronous particle is a stable point situated between $-\pi/2$ and 0[9].

The choice of the synchronous phase delimits a phase acceptance:

– The higher limit ϕ_1 is the phase for which a late particle gets the same energy gain as the synchronous particle:

$$\phi_1 = -\phi_{s0} \Rightarrow \varphi_1 = -2 \cdot \phi_{s0}\,. \tag{76}$$

– At the lower limit ϕ_2, the confinement potential equals the potential at the higher limit (ϕ_1). As the potential is the integral of the force, ϕ_2 is the phase for which the horizontally hatched surface on Fig. 7 equals the vertically hatched one. It can be calculated from the Hamiltonian given in Eq. (75):

$$H_{\varphi w}\left(\varphi = \phi_2 - \phi_{s0}, w = 0\right) = H_{\varphi w}\left(\varphi = \phi_1 - \phi_{s0}, w = 0\right). \tag{77}$$

ϕ_2 is the solution of

$$\left(\sin\phi_2 - \phi_2 \cos\phi_{s0}\right) + \left(\sin\phi_{s0} - \phi_{s0}\cos\phi_{s0}\right) = 0\,. \tag{78}$$

– The choice of the synchronous phase determines also the energy acceptance ΔE corresponding to the difference between the potential energy of a particle with a phase ϕ_1 and that of the synchronous particle. It can also be calculated from the Hamiltonian given in Eq. (75):

$$H_{\varphi w}\left(\varphi = 0, w = \Delta E\right) = H_{\varphi w}\left(\varphi_1 = \phi_1 - \phi_{s0}, w = 0\right), \tag{79}$$

[9] For a positively charged particle, as for a negatively charged one it depends on convention (is $qE_0 > 0$ or $E_0 > 0$?).

giving

$$\Delta E = 2 \cdot qE_0 T\left(\phi_{s0} \cos\phi_{s0} - \sin\phi_{s0}\right). \tag{80}$$

$$\Delta E = \left(\frac{\left(\beta_s \gamma_s\right)^3 \cdot \lambda \cdot mc^2}{\pi} \cdot 2 \cdot qE_0 T\left(\phi_{s0} \cos\phi_{s0} - \sin\phi_{s0}\right) \right)^{\frac{1}{2}}. \tag{81}$$

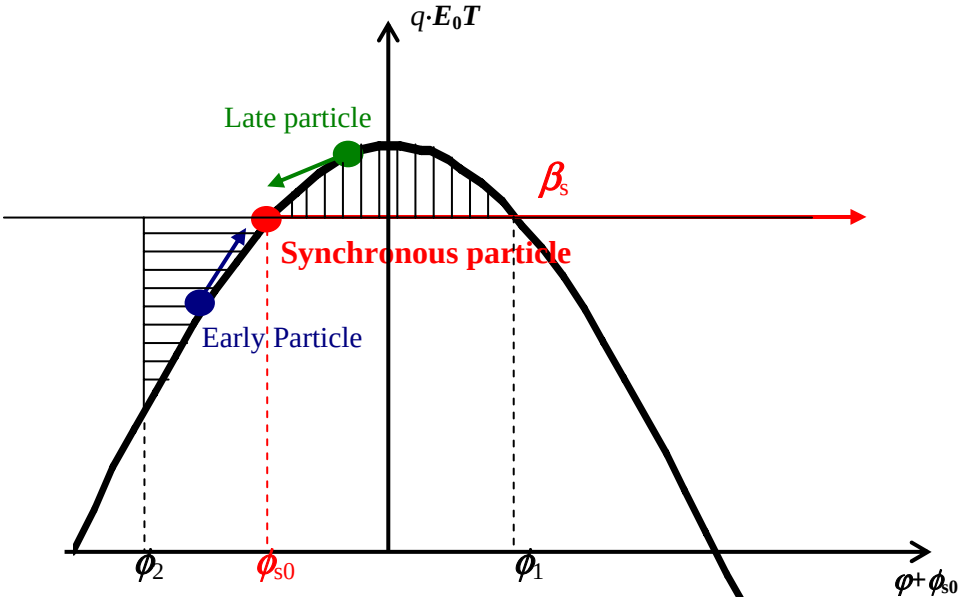

Fig. 7: Energy gain — synchronous particle

The acceptance area in the phase-energy space is called the ***bucket***, its limit is called the ***separatrix***. The energy acceptance ΔE and the phase ϕ_2 are represented as a function of the synchronous phase on Fig. 8.

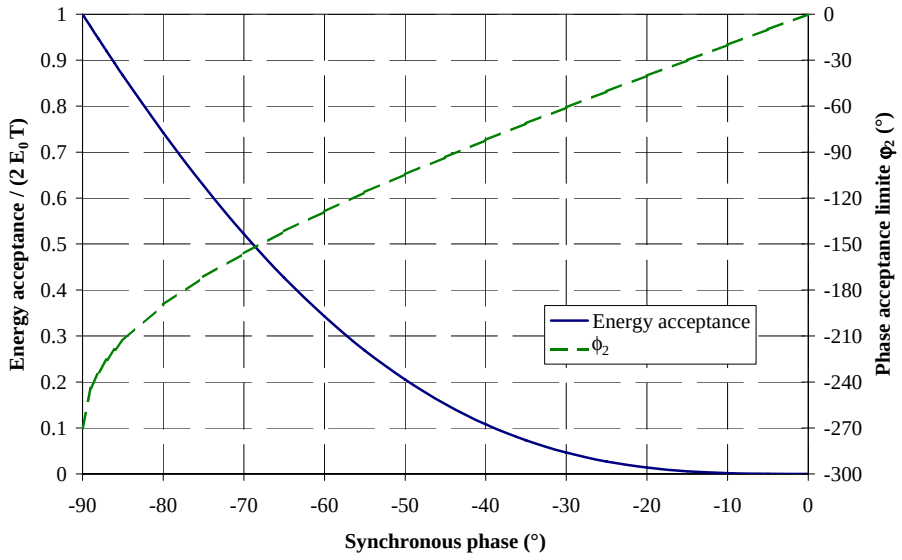

Fig. 8: Bucket dimensions as a function of the synchronous phase

For small phase amplitude oscillations, Eq. (74) becomes

$$\begin{cases} \dfrac{d\varphi}{ds} = -2\pi \cdot \dfrac{w}{(\beta_s\gamma_s)^3 \cdot mc^2 \cdot \lambda} \\ \dfrac{dw}{ds} = q \cdot E_0 T_s \cdot \sin\phi_{s0} \cdot \varphi \end{cases} \tag{82}$$

giving the second-order differential equation of phase evolution:

$$\frac{d^2\varphi}{ds^2} + \frac{2}{\varsigma} \cdot \frac{d\varphi}{ds} + k_z^2 \cdot \varphi = 0\,, \tag{83}$$

with

$$k_z^2 = \frac{2\pi q \cdot E_0 T_s \cdot \sin(-\phi_{s0})}{(\beta_s\gamma_s)^3 \cdot mc^2 \cdot \lambda}\,. \tag{84}$$

Here k_z is the phase advance per metre of the beam core. In periodic structures of period L, $\sigma_z = k_z L$ is the longitudinal core phase advance per lattice.

$$\varsigma = \frac{2}{3} \cdot \frac{\beta_s\gamma_s}{d(\beta_s\gamma_s)/ds}\,. \tag{85}$$

Here ς is the damping length of the core oscillations.

Both ς and the variation of k_z with $\beta_s\gamma_s$ contribute to phase oscillation damping with acceleration. The adiabatic damping of the phase amplitude oscillation φ_a, defined when the contribution of ς is negligible, can be calculated [7]:

$$\varphi_a \propto (\beta_s\gamma_s)^{-3/4}\,. \tag{86}$$

The *Liouville theorem* implies that the energy amplitude oscillation w_a variation is

$$w_a \propto (\beta_s\gamma_s)^{3/4}.$$

The Hamiltonian in linear force then becomes

$$H_{\varphi w} = -\frac{2\pi}{(\beta_s\gamma_s)^3 \cdot mc^2 \cdot \lambda} \cdot \frac{w^2}{2} + q \cdot E_0 T_s \cdot \sin\phi_{s0} \cdot \frac{\varphi^2}{2}\,. \tag{87}$$

The curves for which the Hamiltonian is constant are then ellipses.

4.1.4 Motion in linear force

We have seen that the longitudinal particle motion is basically non-linear, but it can be linearized when the particle phase oscillation amplitude is very small compared to the bucket phase size. The transverse forces are much more linear than the longitudinal one, and the use of linear focusing force is very close to reality, and can be solved analytically.

4.1.4.1 Linear transverse forces

In linacs, the main elements used to transport a beam are the cavities and the quadrupoles. Both these elements induce transverse forces.

Quadrupoles

In a perfect thick lens model, the quadrupole's magnetic field is

$$\begin{cases} B_x = G \cdot y \\ B_y = G \cdot x \end{cases} \tag{88}$$

over a distance ***L*** known as the quadrupole's magnetic length, and 0 outside.

G is the quadrupole gradient (in T/m).

With the paraxial approximation and because a magnetic field does not change the particle energy, the equations of transverse dynamics in quadrupole are then

$$\begin{cases} \dfrac{d\gamma\beta_x}{ds} = \gamma\beta_z \dfrac{dx'}{ds} = -\dfrac{q \cdot G}{mc} x \\ \dfrac{dx}{ds} = x' = \dfrac{\beta_x}{\beta_z} \\ \dfrac{d\gamma\beta_y}{ds} = \gamma\beta_z \dfrac{dy'}{ds} = \dfrac{q \cdot G}{mc} y \\ \dfrac{dy'}{ds} = y' = \dfrac{\beta_y}{\beta_z} \end{cases} . \tag{89}$$

The transverse force is linear in a perfect quadrupole.

Actually, fringe fields and non-perfect hyperbolic poles induce non-linear effects which are generally neglected at first order in linacs.

RF gap

When a particle travels through a cavity, the integration of the effect of the radial electric field and the azimuthal magnetic field can be modelled by a transverse kick, which is linear at second order. This kick modifies the particle transverse momentum:

$$\Delta(\gamma\beta_r) = -\frac{\pi q E_0 TL}{mc^2 \overline{\gamma\beta_z}^2 \lambda} \cdot \sin\phi \cdot \left[r + O\left(r^3\right) \right] = \Delta(\gamma\beta_z) \cdot r' + \gamma\beta_z \cdot \Delta r' . \tag{90}$$

With:

$$\beta_r^2 = \beta_x^2 + \beta_y^2 .$$

The term in r' shows that the particle transverse oscillation is damped by acceleration in accelerating cavities. The dependence on ϕ shows that the transverse dynamics is naturally coupled at second order to the longitudinal one by RF cavities.

4.1.4.2 Motion of a particle in periodic linear force

At first order, the motion of a particle can be linearized and the motion along all directions can be decoupled. The motion equation in the *w* direction (*w* being *x*, *y* or φ) is a solution of a second-order equation:

$$\frac{d^2w}{ds^2}+\frac{A_w}{\gamma\beta_z}\cdot\frac{d\gamma\beta_z}{ds}\cdot\frac{dw}{ds}+k_w(s)\cdot w=0\,. \tag{91}$$

A_w being a constant equal to 1 for $w = x$ or y and 3 for $w = \varphi$.

Now, let us consider that the focusing force is periodic with period $\boldsymbol{S}$, i.e., $k_x(s+S)=k_x(s)$.

Generally, the damping term given by the acceleration is very small and can be considered as a perturbation:

$$\left\langle\left|\frac{A_w}{\gamma\beta_z}\cdot\frac{d\gamma\beta_z}{ds}\cdot\frac{dw}{ds}\right|\right\rangle_S << \left\langle\left|k_w(s)\cdot w\right|\right\rangle_S\,, \tag{92}$$

$\langle a\rangle_S$ giving the average value of quantity a over one lattice period.

With this assumption, the solution of Eq. **(91)** is given by Floquet's theorem:

$$w(s)=\sqrt{\beta_{wm}(s)\cdot I_w/\gamma\beta_z}\cdot\cos\left[\psi_w(s-s_0)+\psi_w(s_0)\right], \tag{93}$$

with $\boldsymbol{\beta_{wm}}$ periodic ($\beta_{wm}(s+S)=\beta_{wm}(s)$), known as the structure's beta function, solution of

$$\frac{d^2\beta_{wm}}{ds^2}+2\cdot k_w(s)\cdot\beta_{wm}-\frac{2}{\beta_{wm}}\cdot\left[1+\frac{1}{4}\cdot\left(\frac{d\beta_{wm}}{dt}\right)^2\right]. \tag{94}$$

$I_w/\gamma\beta_z$, known as the ***Courant–Snyder*** **invariant** (which is actually invariant with no acceleration), and ψ_w the particle phase advance, are defined as:

$$\psi_w(s)=\int_{s_0}^{s}\frac{ds}{\beta_{wm}(s)}\,. \tag{95}$$

In (w, w') phase space, particles are turning around periodic ellipses whose equations are

$$\gamma_{wm}(s)\cdot w^2+2\cdot\alpha_{wm}(s)\cdot w\cdot w'+\beta_{wm}(s)\cdot w'^2=I_w/\gamma\beta_z\,, \tag{96}$$

with

$$\alpha_{wm}(s)=-\frac{1}{2}\frac{d\beta_{wm}(s)}{ds}, \tag{97}$$

and

$$\gamma_{wm}(s)=\frac{1+\left[\alpha_{wm}(s)\right]^2}{\beta_{wm}(s)}\,. \tag{98}$$

The surface of the ellipses decreases as $1/\gamma\beta_z$ which is close to $1/\gamma\beta$ with the paraxial approximation.

The phase advance per lattice $\boldsymbol{\sigma_w}$ defined as:

$$\sigma_w=\psi_w(s+S)-\psi_w(s), \tag{99}$$

gives an idea of how fast the particles are turning around the ellipses. $2\pi/\sigma_w$ is the number of lattice periods after which the particle has made one turn around the ellipse. One can notice that, in linear forces, the phase advance per lattice is the same whatever the particle amplitude.

As an example, let us have a look at a particle motion along one direction in a FODO channel. On Fig. 9, five FODO lattices have been represented. The particle phase advance per lattice is 360°/5 = 72°. The particle position in 2D phase space is represented by the red point in four different positions in the lattice. Each line corresponds to one position:

– 1st line: middle of focusing quadrupole,

– 2nd line: between focusing and defocusing quadrupoles,

– 3rd line: middle of defocusing quadrupole,

– 4th line: between defocusing and focusing quadrupoles.

One observes that lattice after lattice, at the same position, the particle turns around an ellipse. The ellipse shape, whose equation is given by (96), depends on the position within the lattice. This is very important to understand that these ellipses have nothing to do with the beam (no beam has been defined here, but just one particle). These ellipses are defined by the transport channel only.

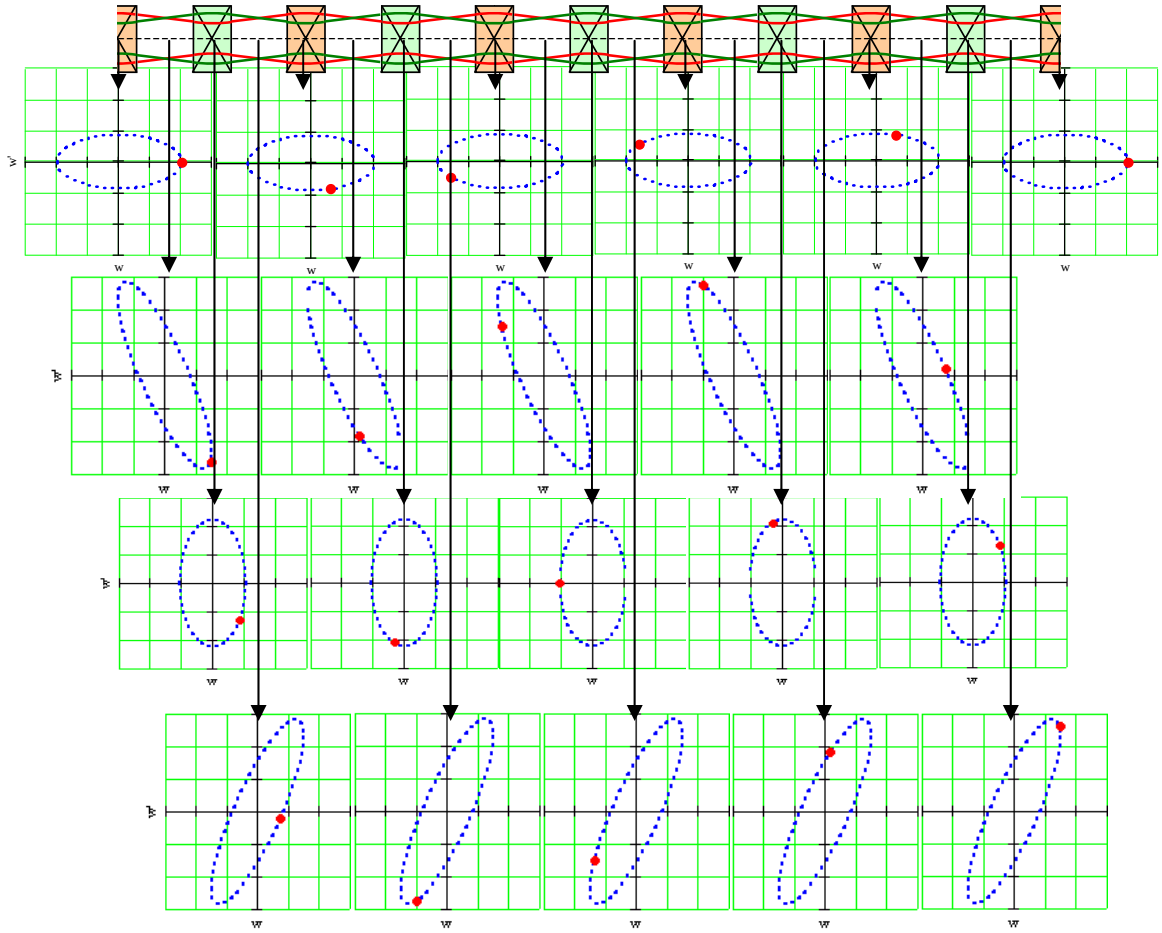

Fig. 9: Particle transport in a FODO channel

As a conclusion, we should keep in mind that a large number of assumptions have been made to obtain that result. The opportunity of each assumption has to be studied very carefully in practical

cases. Nevertheless, the results presented here give a good understanding of the transverse beam dynamics in a linac.

4.2 Beam motion

A beam is a set of particles. The beam motion can then be expressed as the statistical consequence of the individual motion of each particle. Many codes are now transporting beam particles individually, reconstructing beam properties where they are needed. However, some rules should be applied to minimize the degradation of beam optical properties.

4.2.1 Emittances

4.2.1.1 Why?

A beam is a set of billions of particles with different characteristics. It would be very convenient to define and use a simple quantity which would quantify its 'quality' and which would be conserved through a perfect transport and acceleration. How do we define the 'quality' of a beam? Something like: Its ability to perform its goal.

In some accelerators, the goal is to focus the beam on a surface as small as possible, in others, it is to keep it as parallel as possible over a long distance, and in others it is to do both! All these qualities can be quantified by a simple quantity known as the beam emittance[10].

4.2.1.2 What?

Emittance represents the *phase-space volume occupied by beam particles*. The phase space can be either 2D [(x, x'),(y, y'), (phase, energy)], 4D [(x, x', y, y'), (x, x', phase, energy)] or 6D [(x, x', y, y', phase, energy)]. When the phase space is (x, x') or (y, y'), it is called the ***geometric emittance***.

With this definition, a theorem, known as the Liouville theorem, stipulates that the emittance is conserved in conservative forces which depend only on the geometrical dimensions of this phase space (even non-linearly).

4.2.1.3 How?

Let us take a beam in a laminar flow, i.e., all the particles trajectories are parallel to each other (Fig. 10). At a given position s_0, the beam radius is R. All beam particles have a zero slope. In the (x, x') phase space, this beam is a line. The surface it occupies is null, *its emittance is zero*. One metre farther in a drift, the beam size radius is still R. A perfectly laminar beam can be transported without focusing element over an infinite distance. Let us focus this beam with a perfect lens of focal length f, i.e., with a focusing force proportional to the distance from its centre. The beam is focused at distance f to a zero size. A perfectly laminar beam can be focused on an infinitely small surface. In this case, the beam envelope (dashed line on Fig. 10) follows the trajectory of the outside particle.

Let us take a parallel beam with a non-null emittance whose phase-space shape is an ellipse in (x, x') phase space (Fig. 11). At a given position s_0, the beam radius is R. Extreme particles have a zero slope as central particles have a slope between $-x'_0$ and $+x'_0$. The phase-space surface it occupies, its emittance, is non-null. One metre farther in a drift, the beam size radius has increased as the emittance has increased. Let us focus this beam with a perfect lens of focal length f, i.e., with a focusing force proportional to the distance from its centre. The beam is focused at distance f to a non-zero size. The beam size would grow as its emittance grows. The beam envelope is then limited by different particles.

[10] However, it is not unbelievable to define other quantities if the goal is different (like the brightness or the luminosity).

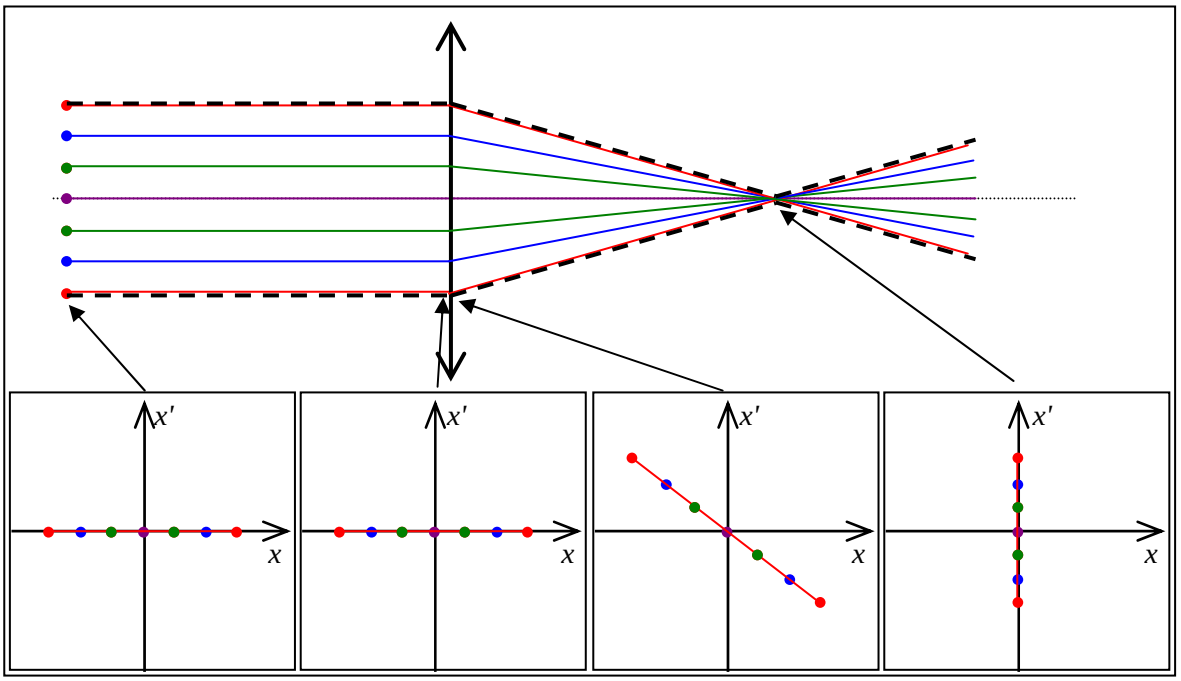

Fig. 10: Particle trajectories in laminar beam

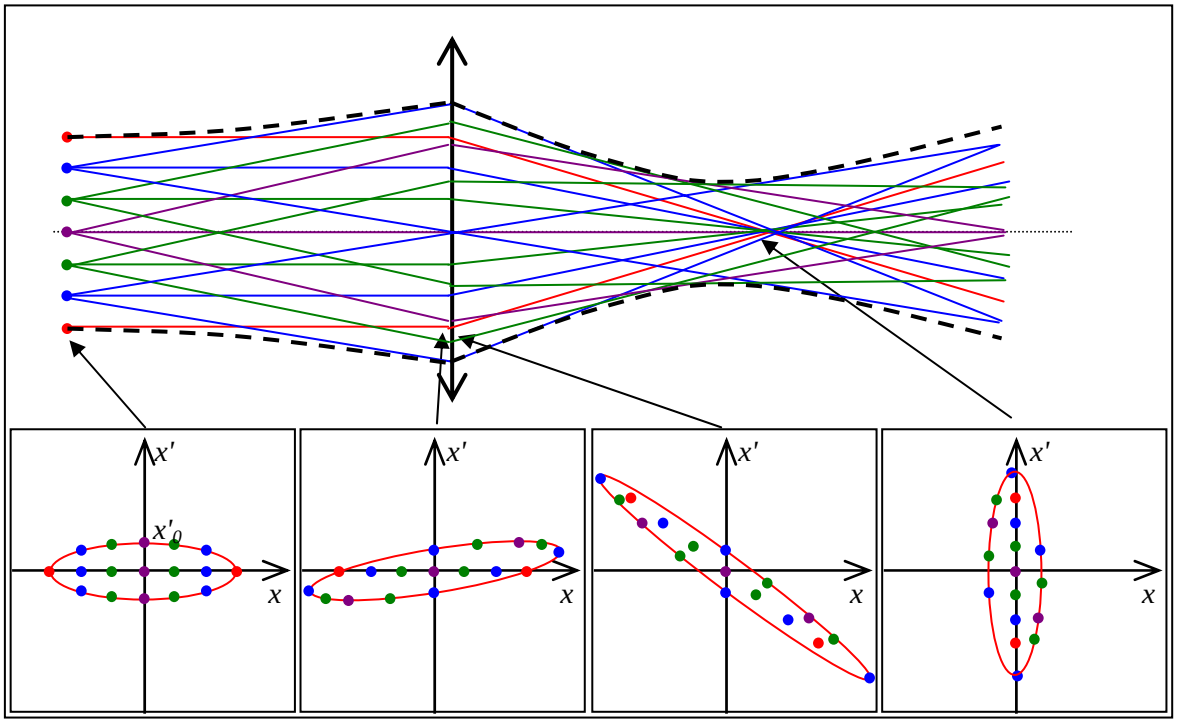

Fig. 11: Particle trajectories in non-zero emittance beam

It is clear that the higher the emittance, the lower the capacity to transport the beam parallel over a long distance and to focus it to a very small size. Moreover, to maintain the beam within a given size, the higher the emittance, the more focusing elements per unit length are needed.

Nevertheless, let us have a look at the focusing of a laminar beam with a non-linear lens (the focusing force is not proportional to the distance from its centre, Fig. 12). It is clear that, through a non-linear lens, the emittance defined as the phase-space volume occupied by the beam is conserved (still zero, a line). However, because the phase-space shape is no longer a straight line, it will be impossible to focus this beam on an infinitely small size or to transport this beam parallel over a infinite distance.

This implies that another definition of emittance is needed to take into account this effect. This 'new' emittance should be

– a phase-space surface,

– non-zero when the beam phase-space distribution is curved,

– easy to calculate whatever the particle distribution in the beam (it is difficult to calculate the phase-space surface occupied by a Gaussian beam which has, per definition, no limit or when only a few of the particles stand very far from the others),

– linked to quantities that can be measured and which have an interest for application.

This quantity is known as the ***root mean squared (r.m.s.) emittance***, linked to the ***root mean squared dimensions*** of the beam.

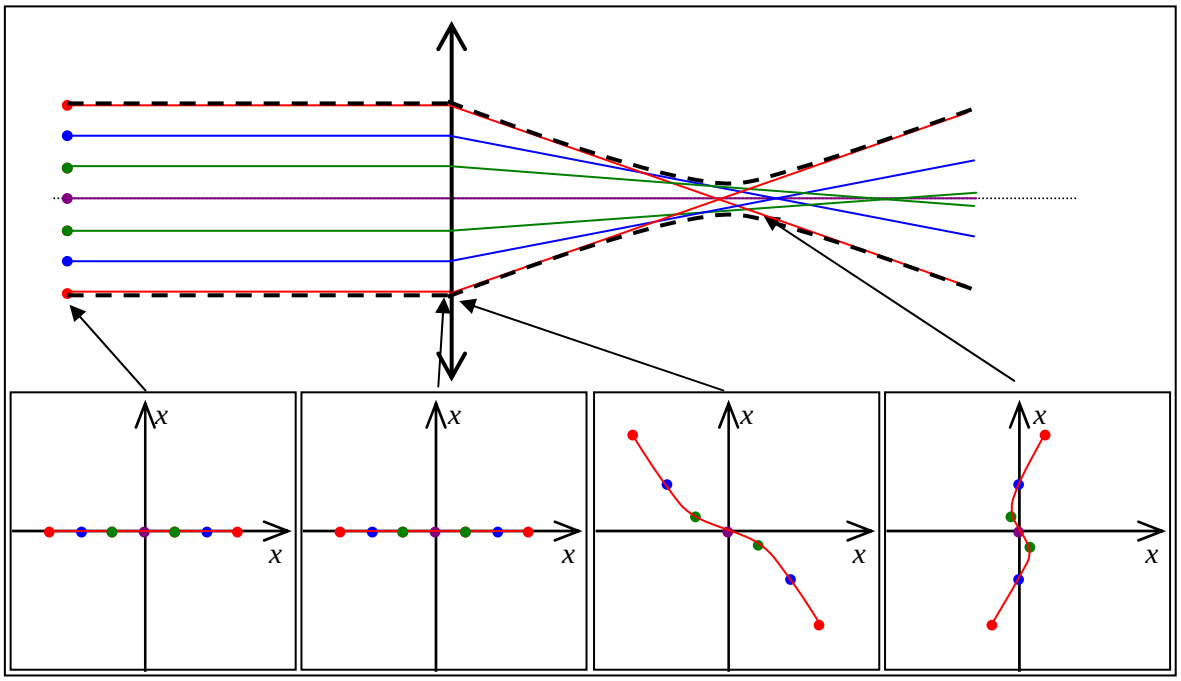

Fig. 12: Particle trajectories in beam focused by non-linear lens

4.2.2 Beam r.m.s. dimensions and Twiss parameters

A bunch has N particles. Its dimensions are defined statistically as follows:

– The beam average position:

$$\langle w \rangle = \frac{1}{N} \sum_{i=1,N} w_i \ , \tag{100}$$

which is the position of its centre of gravity (c.o.g.).

– The beam average slope:

$$\langle w' \rangle = \frac{1}{N} \sum_{i=1,N} w_i' , \tag{101}$$

which is the slope of its c.o.g.

– The beam ***r.m.s. size***:

$$\tilde{w} = \sqrt{\sigma_w} = \sqrt{\left\langle \left(w - \langle w \rangle \right)^2 \right\rangle} = \sqrt{\frac{1}{N} \sum_{i=1,N} \left(w_i - \langle w \rangle \right)^2} , \tag{102}$$

which is the square root of the average square distance of particles from the beam c.o.g. position.

– The beam r.m.s. divergence:

$$\tilde{w}' = \sqrt{\sigma_{w'}} = \sqrt{\left\langle \left(w' - \langle w' \rangle \right)^2 \right\rangle} = \sqrt{\frac{1}{N} \sum_{i=1,N} \left(w_i' - \langle w' \rangle \right)^2} , \tag{103}$$

which is the square root of the average square slope of particles from the beam c.o.g. slope.

– The beam 2D phase-space coupling term is:

$$w w'_{\mathrm{rms}} = \sigma_{ww'} = \left\langle \left(w - \langle w \rangle \right) \cdot \left(w' - \langle w' \rangle \right) \right\rangle , \tag{104}$$

which gives the coupling of the phase-space distribution.

– The beam r.m.s. emittance:

$$\tilde{\varepsilon}_w = \sqrt{\tilde{w}^2 \tilde{w}'^2 - \left\langle \left(w - \langle w \rangle \right) \cdot \left(w' - \langle w' \rangle \right) \right\rangle^2} . \tag{105}$$

Let us meditate a little on the properties of this ‘new’ emittance:

– It has the dimension of a surface in the (*w*, *w'*) phase space.

– When the coupling term is zero, the r.m.s. emittance is simply the product between r.m.s. size and r.m.s. divergence. Otherwise, the emittance is smaller.

– If the beam (*w*, *w'*) phase-space chart is a line whose equation is

$$w' = \begin{vmatrix} k \cdot w \ \ if \ \ |w| \le w_0 \\ 0 \ \ otherwise \end{vmatrix} ,$$

whose surface is zero (laminar beam) its r.m.s. emittance is simply

$$\tilde{\varepsilon}_w = \sqrt{k^2 \cdot \tilde{w}^2 - k^2 \cdot \left\langle \left(w - \langle w \rangle \right) \right\rangle^2} = 0 ,$$

whatever the value of k or w_0.

– When a particle is transported through a linear transformation

$$\begin{pmatrix} w \\ w' \end{pmatrix}_1 = \begin{pmatrix} M_{11} & M_{12} \\ M_{21} & M_{22} \end{pmatrix} \cdot \begin{pmatrix} w \\ w' \end{pmatrix}_0 ,$$

it is easy to show that

$$\tilde{\varepsilon}_{w1} = \sqrt{M_{11} \cdot M_{22} - M_{12} \cdot M_{21}} \cdot \tilde{\varepsilon}_{w0} .$$

The emittance is conserved when the transfer matrix determinant is one (quadrupoles, drifts, etc.).

– When a beam is accelerated from a reduced momentum $\gamma\beta_0$ to $\gamma\beta_1$, the transverse transfer matrix determinant of the accelerating element is not 1 but : $\gamma\beta_0/\gamma\beta_1$. This effect is due to the increase of longitudinal momentum without variation of the transverse one leading to a reduction of the particle slope by $\gamma\beta_0/\gamma\beta_1$. The r.m.s. emittance which is conserved even with acceleration is called the ***normalized r.m.s. emittance*** and its expression (in paraxial approximation) is

$$\tilde{\varepsilon}_{wn} = \beta\gamma \cdot \tilde{\varepsilon}_w . \tag{106}$$

– Because it is linked to average dimensions of the beam, the r.m.s. emittance is smaller than the surface of the smallest ellipse enclosing all the beam particles. The ratio between this 'total' emittance and the r.m.s. emittance depends on the particle distribution.

The beam *Twiss parameters* are then deduced from the beam r.m.s. dimensions:

$$\tilde{\beta}_w = \frac{\tilde{w}^2}{\tilde{\varepsilon}_w} , \qquad \tilde{\gamma}_w = \frac{\tilde{w}'^2}{\tilde{\varepsilon}_w} , \qquad \tilde{\alpha}_w = -\frac{\left\langle \left(w - \langle w \rangle \right) \cdot \left(w' - \langle w' \rangle \right) \right\rangle}{\tilde{\varepsilon}_w} . \tag{107}$$

$$\tilde{\gamma}_w \cdot w^2 + 2 \cdot \tilde{\alpha}_w \cdot w \cdot w' + \tilde{\beta}_w \cdot w'^2 = n \cdot \tilde{\varepsilon}_w \tag{108}$$

is the equation of an ellipse in (w, w') phase-space fitting the best the particle distribution.

Generally, at least 90% of the bunched-beam particles occupy an ellipse with $n = 5$[11]:

Generally, at least 90% of the continuous-beam particles occupy an ellipse with $n = 4$[11]:

The parameter w can be x, y, z or φ. Figure 13 is represented by the phase-space 2D projections of a beam modelled by ~100 000 macro-particles. Ellipses in red correspond to ellipses calculated with Eq. (108) with $n = 5$. They contain, in this example, 92% of the particles.

[11] If the beam distribution were a uniform ellipse in real space, 100% of the particles would occupy this ellipse.

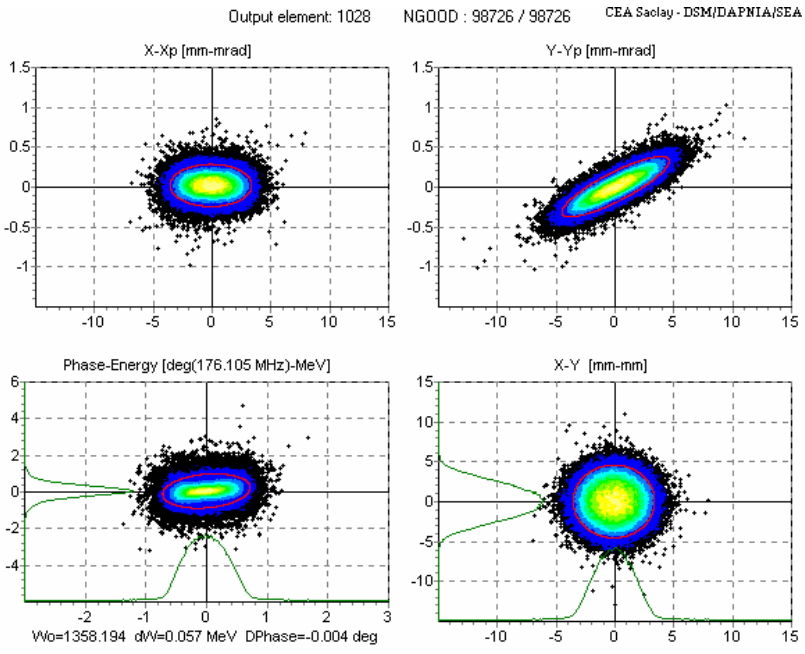

Fig. 13: Phase-space beam distribution and Twiss parameters

4.2.3 Matched/mismatched beam

A beam is matched when its Twiss parameters at a given position *s* correspond to the transport channel periodic Courant–Snyder parameters.

Matched beam :	Beam's Twiss parameters = Channel's Courant–Snyder parameters.

In this condition, the same beam phase-space shape is reproduced period after period. The beam envelope evolution with *s* is periodic and the smoothest possible. On Fig. 14 has been represented the evolution of beams in the same FODO channel as in Fig. 9. In the middle line are plotted the ellipses representing the beams in the phase space at the focusing quadrupole centre. The dashed black circle represents a particle trajectory in this phase space. One matched (in continuous red) and two mismatched (in dashed pink and dotted blue) beams are represented. One particle of each beam has also been represented.

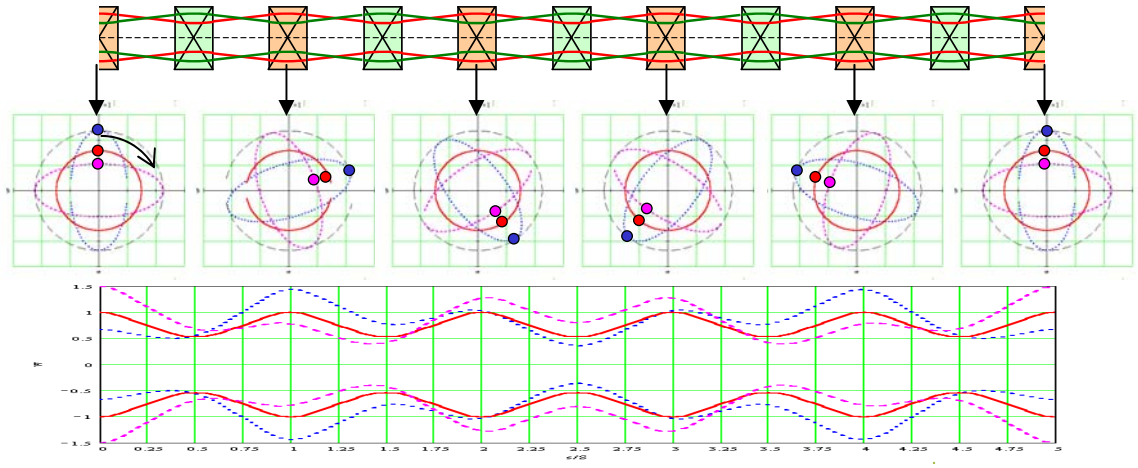

Fig. 14: Matched and mismatched beam in FODO channel

The matched beam ellipse is periodic, as one particle is replaced by an other one. Its envelope (last line) is periodic with the lattice period ***L***.

The mismatched beam ellipses sweep a bigger area (dashed-black circle) than the beam ellipse surfaces. Their envelope period is greater than the lattice period. Its oscillation is a combination of two oscillations with two different periods: one is the lattice period *L*, the other is $2\pi/\sigma_w \cdot L$, σ_w being the channel phase advance per lattice.

– When the *force is linear* (Fig. 15), all particles oscillate in the phase-space with the same period (i.e. the same phase advance per lattice). The beam phase-space distribution changes lattice after lattice, but its emittance is kept constant.

– When the *force is non-linear* (Fig. 16) [external force or force induced by space-charge (Coulomb interactions between beam particles)], the particle's phase-advance per lattice depends on its oscillation amplitude. Beam particles no longer turn all at the same angular speed in the phase space, and an apparent emittance growth is observed[12]. This effect is known as beam filamentation (Fig. 17). After a long time (many particle betatron periods), the phase space swept by the beam is completely full of particles. The apparent emittance is higher.

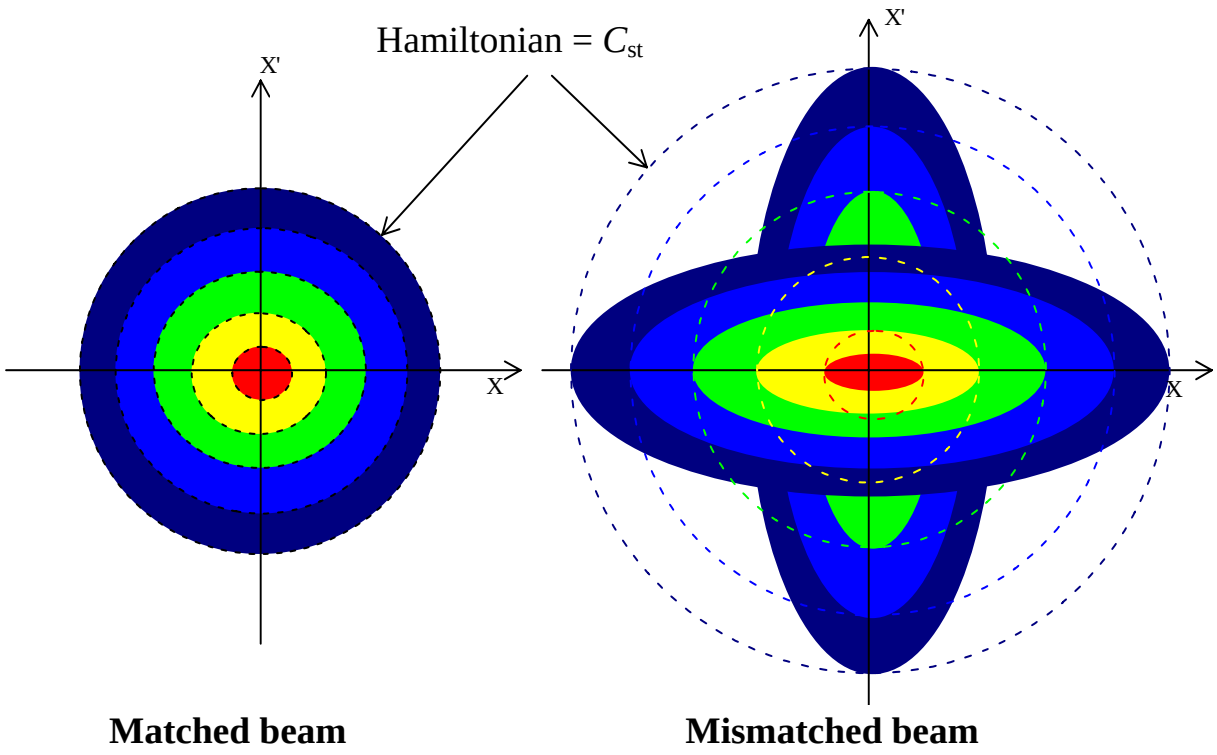

Fig. 15: Matched (left) and mismatched (right) beam in linear forces

[12] Even if the phase-space area occupied by the particle is kept constant (Liouville's theorem applies).

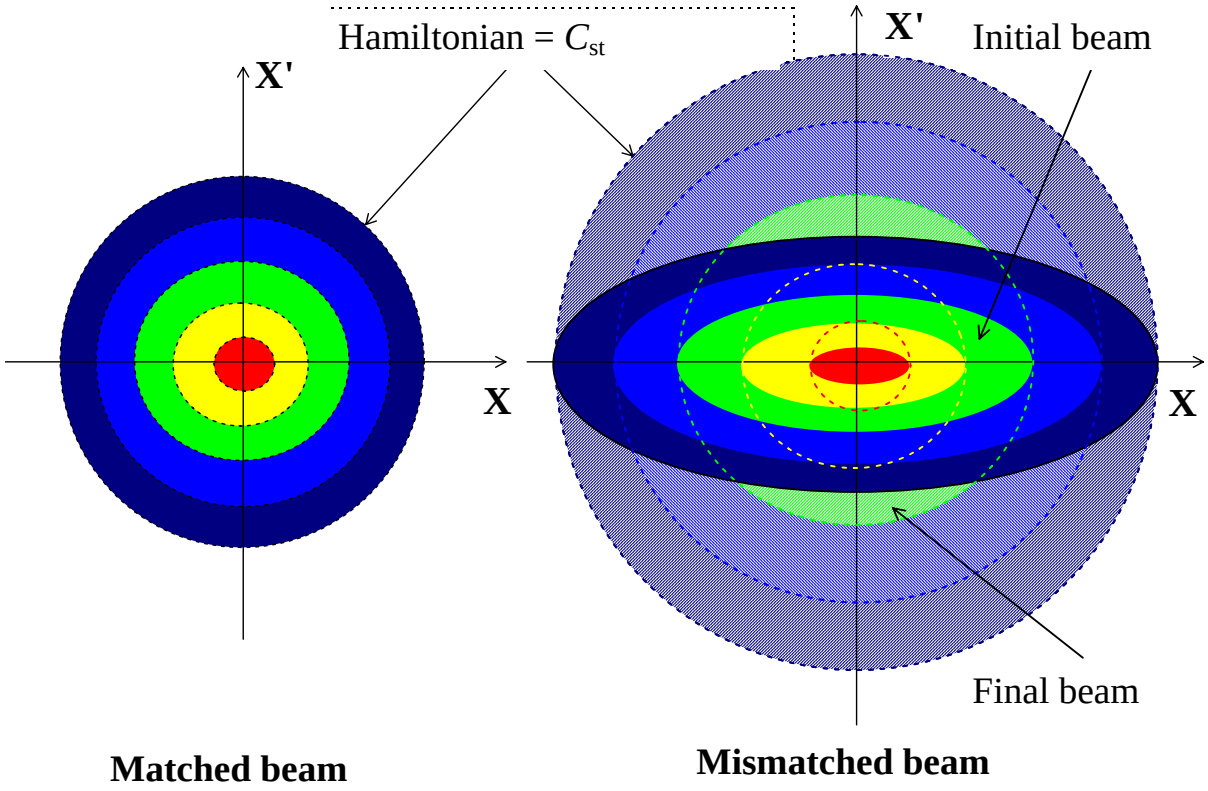

Fig. 16: Matched (left) and mismatched (right) beam in non-linear forces

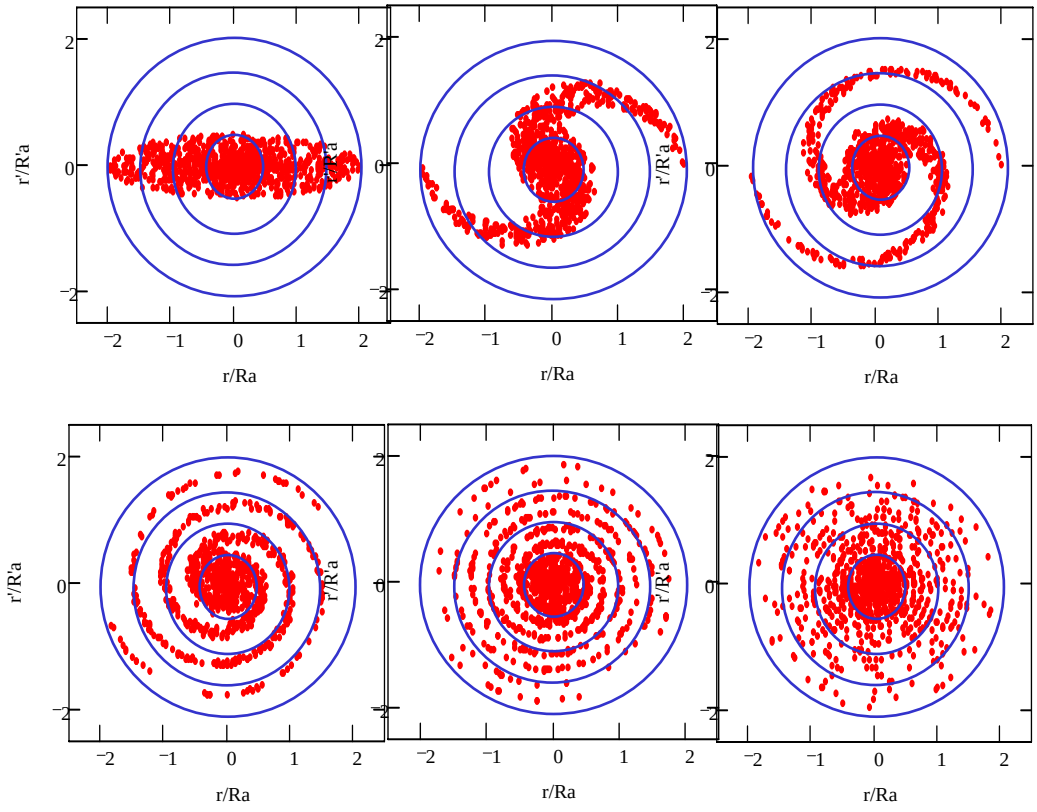

Fig. 17: Filamentation of mismatched beam in non-linear force

5 Conclusion

This paper is a short introduction containing the first basic notions useful to lightly touch upon linacs. A better understanding cannot be obtained without tackling subjects like general beam dynamics, existing structures, RF control, space-charge effects, or resonances. Motivated students are strongly advised to read Thomas Wangler's book [2].

Acknowledgements

Many thanks to Tom Wangler for his wonderful and very useful book on linacs and his encouragement, and to my colleagues Romuald Duperrier and Didier Uriot for their help.

References

[1] P.M. Lapostolle and A.L. Septier (Eds) *Linear Accelerators* (North Holland, Amsterdam, 1970).

[2] T.P. Wangler, *Principles of RF Linear Accelerators* (Wiley, New York, 1998).

[3] *RF Engineering for Particle Accelerators*, CERN Accelerator School, Oxford, UK, 3–10 April 1991, CERN 92-03, 2 vols.

[4] M. Weiss, Introduction to RF linear Accelerators, CERN Accelerator School, Fifth General Accelerator Physics Course, Jyväskylä, Finland, 7–18 september 1992, CERN 94-01, 2 vols.

[5] T. Nishikawa, Transients and beam loading effect, *Linear Accelerators,* P.M. Lapostolle and A.L. Septier (Eds) (North Holland, Amsterdam, 1970).

[6] A. Carne *et al.*, Numericals methods. Acceleration by a gap, *Linear Accelerators* P.M. Lapostolle and A.L. Septier (Eds) (North Holland, Amsterdam, 1970).

[7] J. Le Duff, Dynamics and acceleration in linear structures, CERN Accelerator School, Fifth General Accelerator Physics Course, Jyväskylä, Finland, 7–18 September 1992, CERN 94-01, 2 vols.